Results in Engineering 18 (2023) 101227

Contents lists available at ScienceDirect

Results in Engineering

journal homepage: www.sciencedirect.com/journal/results-in-engineering

An impact of radiation on laminar flow of dusty ternary nanofluid over porous stretching/shrinking sheet with mass transpiration

U.S. Mahabaleshwar [a], T. Maranna [a], L.M. Pérez [b], G.V. Bognár [c], H.F. Oztop [d,e,*]

[a] Department of Studies in Mathematics, Shivagangotri, Davangere University, Davangere, 577 007, India
[b] Departamento de Física, FACI, Universidad de Tarapacá, Casilla 7D, Arica, Chile
[c] Institute of Machine and Product Design Faculty of Mechanical Engineering, Informatics University of Miskolc, Miskolc-Egyetemváros, 3515, Miskolc, Hungary
[d] Department of Mechanical Engineering, Technology Faculty, Firat University, Elazig, Turkey
[e] Department of Medical Research, China Med. University Hospital, China Med. University, Taichung, Taiwan

ARTICLE INFO

Keywords:
Dusty fluids
Ternary nanofluid
Radiation
ODE
Porous media
Mass suction/injection

ABSTRACT

The goal of current research is to determine the laminar boundary layer problem for the two-dimensional flow of ternary dusty nanoparticles through a porous stretching/shrinking sheet in the presence of radiation and mass transpiration. Generalized partial differential equations are converted to nonlinear ordinary differential equations after demonstrating an appropriate similarity transformation. Exact solutions are subsequently provided for the resulting system of equations. The development of ternary dusty nanofluids has significantly improved the heat transmission process for manufacturing and industrial applications, as well as in nanotechnology research. The influence of the various interesting parameters on the flow and heat transfer is analyzed and discussed in detail through plotted graphs. It was found that the basic similarity equations admit two phases for both stretching/shrinking surfaces. Graphs are used to illustrate the findings of this work. We found that the velocity fields increase with an increase in the inverse Darcy number value for the case stretching sheet while opposite effects can be observed in the shrinking case. Moreover, the magnitude of particle interaction parameter enhances as the solution domain raises. The findings disclose that the performance of ternary nanofluid phase heat transfer is improved compared to dusty phase performance.

1. Introduction

Recently, numerous areas of engineering and technology have greatly benefited from the study of dusty fluid flow. The findings on dusty flows are beneficial in the research of air pollution, vehicle emissions of smoke and other pollutants, industrial effluent emissions, combustion, paint sparing, capillary blood flow, and other problems. Dust particles impact on a gas's ability to sustain consistency in laminar flow is investigated by Saffaman et al. [1]. Initially discussed the movement of a boundary layer over a persistent, thick surface that was moving steadily, as described by Sakiadis et al. [2]. Michel et al. [3] analyzed a dusty gas flow with uniformly distributed dust particles that was covering the edge of a solid plane, there is a semi-infinite space. Crane et al. [4] developed a closed-form effective approach by extending the Sakiadis problem to a stretching surface.

In order to build ternary nanofluids, three different kinds of nanoparticles with various chemical and physical properties are immersed in a base fluid, and these are the nanosized particles. Such nanoparticles have been demonstrated to effectively develop the base fluid's thermal conductivity and heat transfer capabilities. Earlier, Chaoi et al. [5] verified the theory that nanoscale particles should be suspended in base fluids to increase their thermal conductivity. Additionally, the influence of radiation on the magnetohydrodynamic flow of couple stress fluids, nanofluids, casson hybrid nanofluids, and CNTs-water dependent nanofluids was extensively studied by Mahabaleshwar et al. [6–9]. In terms of frequency of occurrence, metallic nanoparticles like metal nitride, metallic carbide, metallic oxides, carbon-based materials (graphite, MWCNTs, CNTs), metal oxides (Al_2O_3, CuO, Fe_2O_3), and (Cu, Ag), were the most common forms of nanoparticles. Furthermore, the structure, size, shape, and solid volume fractions of the nanofluids are all important aspects in optimizing the conductivity of hybrid nanofluids.

The mathematical models of Buongiorno et al. [10] and Tiwari et al. [11] are commonly used for the characterization of boundary layer flow in nanofluids. Ternary hybrid nanofluid flows are exposed to magnetic moments as well as a heat source and sink on a hot wall, is investigated

* Corresponding author. Department of Mechanical Engineering, Technology Faculty, Firat University, Elazig, Turkey.
E-mail address: hfoztop1@gmail.com (H.F. Oztop).

https://doi.org/10.1016/j.rineng.2023.101227
Received 10 April 2023; Received in revised form 20 May 2023; Accepted 5 June 2023
Available online 7 June 2023

Nomenclature

List of Symbols Descriptions S·I. Units

A_1, A_2, A_3, A_4	Constants, $(-)$
b	Constant, $(-)$
c	Constant, $(-)$
C_p	Specific heat, $(JK\ g^{-1}K^{-1})$
d	Stretching/shrinking parameter, $(-)$
Da	Darcy number $(-)$
K_1	Drag coefaficient, $(-)$
k	Permeability, (NA^{-2})
k^*	Mean absorption coefficient, $(-)$
m	Mass, (Kg)
N_r	Radiation parameter, $(-)$
q_r	Heat flux, (Wm^{-2})
Pr	Prandtl number $(-)$
T	Fluid temperature, (K)
T_p	Dusty fluid temperature, (K)
T_∞	Ambient temperature, (K)
u, v	Velocities along x and y-directions, (m/s)
u_p, v_p	Dusty fluid velocity components, (m/s)
V_c	Mass transpiration, $(-)$
x	Horizontal axis, $(c/\ m)$
y	Vertical axis, $(c/\ m)$

Greek symbols

β	Fluid particle interaction variable, $(-)$
φ	Fluid nanoparticle volume fraction ratio, $(-)$
φ_1	Silver nanoparticle volume fraction, $(-)$
φ_2	SWCNTs nanoparticle volume fraction, $(-)$
φ_3	Graphene nanoparticle volume fraction, $(-)$
ρ	Density (Kg/m^3)
σ^*	Stefan-Boltzmann constant, $(Wm^{-2}K^{-4})$
ν_{tnf}	Kinematic viscosity of ternary nanofluid, (m^2s)
ρ_{tnf}	Density o the ternary nanofluid, (Kgm^{-3})
κ_{tnf}	Thermal conductivity of ternary nanofluid, $(Wm^{-1}\ K^{-1})$
κ_{bf}	Thermal conductivity of base fluid, $(Wm^{-1}\ K^{-1})$
(ρC_p)	Heat capacitance of fluid, $(JK\ g^{-1}K^{-1})$
η	Dimensionless variable, $(-)$
θ	Temperature similarity variable for fluid, $(-)$
Φ	Temperature similarity variable for dusty fluid, $(-)$
Λ	Mass number $(-)$

Subscripts

bf	Base fluid, $(-)$
nf	Nanofluid, $(-)$
tnf	Ternary nanofluid, $(-)$

Abbreviations

PDEs	Partial differential equations, $(-)$
ODEs	Ordinary differential equations, $(-)$
BL	Boundary layer $(-)$
RANS	Reynolds averaged Navier-Stokes, $(-)$

by Animasaun et al. [12]. Heat transfer in ternary nanoparticles (TiO_2–SiO_2–Al_2O_3–H_2O) flowing along a stretched surface is theoretically examined by Manjunatha et al. [13]. Focusing on the impacts of relative velocity and heat transfer of nanoparticles of three different configurations on the transportation induced by wall stretching is analyzed by Animasaun et al. [14]. Effects of mass transpiration and radiation on it, as well as through a nonlinear stretching sheet, HNF flow with mass transfer occurs in permeable media, is described by Anush et al. [15]. Recently, Hatami et al. [16,17] worked analytically and numerically on the flow of non-Newtonian fluid, micropolar fluid, and transmission of heat in porous medium as well as vertical flat plates. In their research, Siddheshwar et al. [18,19], looked at the flow of magnetohydrodynamic viscoelastic fluid and the transmission of heat across stretched surfaces and permeable media. He also discussed the characteristics of radiation and heat sources. Modelling the BL flow of a 2-phase dusty fluid across a stretched/contractible sheet has been depicted by Turkyilmazoglu et al. [20]. Naramgari et al. [21] looked into the MHD flow of a dusty nanofluid with a volume proportion of dust particles across a stretched surface. A porous stretched sheet is passed by boundary layer streams of an immiscible conductive fluid, is studied by Vinaykumar et al. [22]. Gao et al. [23] investigated the statistical activity of the scaling dispersion rate transmission of the reaction progression parameter and its modelling within the setting of the Reynolds averaged Navier-Stokes simulation.

For instance, Obaidi et al. [24,25] investigated the impact of various twisted tape insert configurations on fluid flow characteristics, pressure drop, thermohydraulic performance, and thermal transfer improvements in the 3D circular tube. Other valuable references on thermal flow structure and performance heat transfer in three-dimensional circular tube/pipe can be found in Refs. [26–31]. The researcher [32,33] works on hydromagnetic Williamson fluid flow and Forchheimer sisko nanofluid flow through a radiative surface. Recently, Souayeh et al. [34] depicted the flow of a dusty ternary nanofluid over a stretching sheet. Roy et al. [35] address the properties of the flow and heat transfer of a dusty hybrid nanofluid flow across an unstable shrinking sheet in the presence of a magnetic field. Noorzehan et al. [36] analyses the influences of the suction parameter and the fluid-particle interaction parameter on the boundary layer of the dusty fluid towards the stretching sheet.

Although there appear quite a large number of studies on the considered problem published in the open literature, some of them as per cited above, none deals with an analytical approach nor a proper analysis has been fulfilled taking into account the mass flow addition into the boundary layer flow resulted from a two-phase dusty fluid flow model. The governing PDEs are converted into nonlinear ODEs. Analytical method is employed to find the solutions of momentum and temperature equation. In current paper, the effects of several physical characteristics, including the mass transpiration parameter, the fluid interaction temperature parameter, Eckert number, Prandtl number, sold volume fraction and radiation parameters are also studied.

The novelty of the current paper is, therefore to investigate the boundary layer flow of two-phase dusty ternary nanofluid model over porous stretching/shrinking sheet when mass transfer is present. Extracting exact analytical unique/multiple solutions is the main target. It is proved that the two-phase flow and heat can be represented via simple but ingeniously smart formulae from which knowledge can be gained for the momentum and thermal layer behaviors in both phases, and hence exact information on the momentum and thermal boundary layer can be obtained. Moreover, the findings of the current study must be described in the context of water that is carrying spherical silver nanoparticles, cylinder-shaped single-walled CNT particles, and platelet-shaped graphene nanoparticles. The current work has numerous industrial applications and argues with the work of [20,39]. The presented solutions not only are of significance to the practical applications but they also serve to the further research in the ongoing topic involving more complex physical phenomena, as inferred from the aforementioned, more recent articles in the field. We should mention priorly that Mathematica software is used to generate the presented results.

2. Mathematical model and solution

Consider steady, two dimensional and incompressible viscous laminar flow of dusty ternary nanofluid over a porous stretching/shrinking sheet. Presume sheet direction is horizontal with the x-axis and y-axis is the direction normal to the stretching sheet as see in Fig. 1 he stretching/shrinking sheet is parallel to the $y=0$ plane. And its velocity is assumed as $u_w(x) = cx,\ c>0$, for stretching sheet case and $c<0$ for shrinking sheet. The ternary hybrid nanofluid embodies three kinds of nanoparticles i.e. silver, SWCNT, and Graphene with diverse nanoparticle shapes of spherical, cylindrical, and platelet, respectively.

2.1. Governing equations

The following essential equations govern the fluids boundary layer flow [20,21,39,57] as a follow.

2.1.1. Fluid phase

$$\frac{\partial u}{\partial x}+\frac{\partial v}{\partial y}=0, \tag{1}$$

$$u\frac{\partial u}{\partial x}+v\frac{\partial u}{\partial y}=\nu_{tnf}\frac{\partial^2 u}{\partial y^2}+\frac{K_1N}{\rho_{tnf}}(u_p-u)-\frac{\nu_{tnf}}{k}u, \tag{2}$$

2.1.2. Dusty fluid phase

$$\frac{\partial u_p}{\partial x}+\frac{\partial v_p}{\partial y}=0, \tag{3}$$

$$u_p\frac{\partial u_p}{\partial x}+v_p\frac{\partial u_p}{\partial y}=\frac{K_1}{m}(u-u_p), \tag{4}$$

$$u\frac{\partial T}{\partial x}+v\frac{\partial T}{\partial y}=\frac{\kappa_{tnf}}{(\rho C_p)_{tnf}}\frac{\partial^2 T}{\partial y^2}+\frac{\rho_p c_m}{(\rho C_p)_{tnf}\tau_T}(T_p-T)+\frac{\rho_p}{\tau_v(\rho C_p)_{tnf}}(u_p-u)^2-\frac{1}{(\rho C_p)_{tnf}}\frac{\partial q_r}{\partial y}, \tag{5}$$

$$u_p\frac{\partial T_p}{\partial x}+v_p\frac{\partial T_p}{\partial y}=-\frac{\rho_p C_m(T_p-T)}{\tau_T}, \tag{6}$$

Boundary conditions include fluid and dusty particles [20,21,39] are

$$\left.\begin{array}{ll} u=u_w(x)=cx,\ v=v_w,\ T=T_w(x)=T_\infty+bx^2 & \text{at}\quad y=0 \\ u\to 0,\ u_p\to 0,\ v_p\to v,\ T\to T_\infty,\ T_p\to T_\infty & \text{at}\quad y=\infty \end{array}\right\}, \tag{7}$$

where (u,v) and (u_p,v_p) represents the velocity components of fluid and dusty fluid phases along (x,y) directions respectively. The fluid as well as dusty fluids are both at a temperature of T and T_p, ternary nanofluid kinematic viscosity is ν_{tnf}, the density of the fluid is ρ, in a given volume, the quantity of nanoparticles is N, coefficient of drag or resistance of stokes is K_1, dust particle mass is to be m, thermal conductivity of fluid is k_{tnf}, dynamic viscosity of the ternary nanofluid is μ_{tnf}, ρ_{tnf} is the ternary nanofluids effective density, dust particles and ternary nanofluids specific heat coefficients are c_p and c_m, heat equilibrium denotes as τ_T, and relaxation time parameter of the dust fluid is $\tau_v=\frac{m}{K_1}$. (ρC_p) is the ternary Nanofluids heat capacitance, and k is the permeability of the fluid flow.

3. Similarity transformation

The following similarity transformations are introduced to transform the governing PDEs into a set of ODEs [20,21,39].

$$\left.\begin{array}{l} u=|c|\,xf'(\eta),\ v=-\sqrt{|c|\nu_f}f(\eta),\ \eta=\sqrt{\dfrac{|c|}{\nu_f}}y, \\ u_p=|c|\,xF'(\eta),\ \nu_p=-\sqrt{\nu_f|c|}F(\eta), \\ \theta=\dfrac{T-T_\infty}{T_w-T_\infty},\ \Phi=\dfrac{T_p-T_\infty}{T_w-T_\infty}. \end{array}\right\}, \tag{8}$$

here η is the similarity variable, f and F are the stream functions for fluid and dusty fluid. $c>0$ is constant with wall mass transfer velocity is $v_w=-\sqrt{\nu_f|c|}V_c$..

Employing the Rosseland approximation, the value of radiative heat

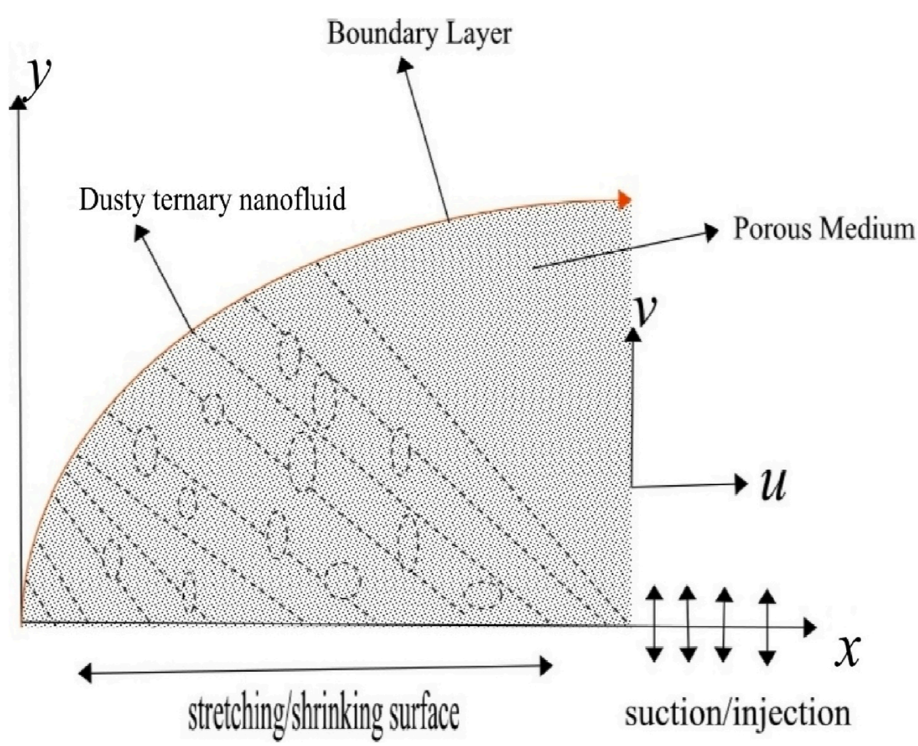

Fig. 1. Diagramatic representation of the fluid flow.

flux [37–43,55] is stated as

$$q_r = -\frac{4\sigma^*}{3k^*}\frac{\partial T^4}{\partial y}, \tag{9}$$

where k^* and σ^* stand for the mean absorption coefficient and Stefan –Boltzman constant, respectively. If the temperature difference inside the flow is sufficiently small, we can express the form using the Taylor expansion and ignore the higher order terms as a linear function of temperature.

$$T^4 \cong 4T_\infty^3 - 3T_\infty^4, \tag{10}$$

from Eqn. (9) and Eqn. (10) we have following form

$$\frac{\partial q_r}{\partial y} = -\frac{16\sigma^* T_\infty^3}{3k^*}\frac{\partial^2 T}{\partial y^2}, \tag{11}$$

now Eqn. (5) and Eqn. (6) rewritten as follows

$$u\frac{\partial T}{\partial x} + v\frac{\partial T}{\partial y} = \frac{k_{tnf}}{(\rho C_p)}\frac{\partial^2 T}{\partial y^2} + \frac{\rho_p c_m}{\tau_T(\rho C_p)}(T_p - T) + \frac{\rho_p}{\tau_v(\rho C_p)}(u_p - u)^2 + \frac{16\sigma^* T_\infty^3}{3k^*}\frac{\partial^2 T}{\partial y^2}, \tag{12}$$

$$u_p\frac{\partial T_p}{\partial x} + v_p\frac{\partial T_p}{\partial y} = -\frac{(T_p - T)}{\tau_T} + \frac{16\sigma^* T_\infty^3}{3k^*}\frac{\partial^2 T}{\partial y^2}, \tag{13}$$

According to a few researchers [44,45] advised, the ternary nanofluid quantities of viscosity as well as thermal conductivity are,

$$\mu_{tnf} = \frac{\mu_{nf_1}\varphi_1 + \mu_{nf_2}\varphi_2 + \mu_{nf_3}\varphi_3}{\varphi}, k_{tnf} = \frac{k_{nf_1}\varphi_1 + k_{nf_2}\varphi_2 + k_{nf_3}\varphi_3}{\varphi}, \tag{14}$$

Due to the fact that the structure of the nanoparticles not only affect the density as well as heat capacity in ternary nanofluids, heat capacitance and density quantities are [46,56].

$$\rho_{tnf} = (1 - \varphi_1 - \varphi_2 - \varphi_3)\rho_{bf} + \varphi_1\rho_{sp_1} + \varphi_2\rho_{sp_2} + \varphi_3\rho_{sp_3}, \tag{15}$$

Kalidasan et al. [47] specified thermal capacity of ternary nanofluid quantities are follow

$$(\rho C_p)_{tnf} = (1 - \varphi_1 - \varphi_2 - \varphi_3)(\rho C_p)_{bf} + \varphi_1(\rho C_p)_{sp_1} + \varphi_2(\rho C_p)_{sp_2} + \varphi_3(\rho C_p)_{sp_3}, \tag{16}$$

with $\varphi = \varphi_1 + \varphi_2 + \varphi_3,$.

φ_1 is the spherical silver nanoparticles volume, the cylindrical SWCNTs nanoparticle volume is to be φ_2, platelet graphene nanoparticles volume is represented by φ_3.

Viscosity and thermal conductivity values for spherical nanoparticles [56] are

$$\frac{\mu_{tnf_1}}{\mu_{bf}} = 1 + 2.5\varphi + 6.2\varphi^2, \frac{\kappa_{tnf_1}}{\kappa_{bf}} = \left(\frac{\kappa_{sp_1} + 2\kappa_{bf} - 2\varphi(\kappa_{bf} - \kappa_{sp_1})}{\kappa_{sp_1} + 2\kappa_{bf} + \varphi(\kappa_{bf} - \kappa_{sp_1})}\right), \tag{17}$$

Thermal conductivity and viscosity values for cylindrical nanoparticles [52] are

$$\frac{\mu_{tnf_2}}{\mu_{bf}} = 1 + 13.5\varphi + 904.4\varphi^2, \frac{k_{tnf_2}}{k_{bf}} = \left(\frac{k_{sp_2} + 3.9k_{bf} - 3.9\varphi(k_{bf} - k_{sp_2})}{k_{2sp_2} + 3.9k_{bf} + \varphi(k_{bf} - k_{sp_2})}\right), \tag{18}$$

for platelet nanoparticles, viscosity and thermal quantities [52] are

$$\frac{\mu_{tnf_3}}{\mu_{bf}} = 1 + 37.1\varphi + 612.6\varphi^2, \frac{k_{tnf_3}}{k_{bf}} = \left(\frac{k_{sp_3} + 4.7k_{bf} - 4.7\varphi(k_{bf} - k_{sp_3})}{k_{2sp_3} + 4.7k_{bf} + \varphi(k_{bf} - k_{sp_3})}\right), \tag{19}$$

Eqn. (1) is fulfilled and equations for the two-phase fluid flow with heat transfer that have been transformed are:

$$\frac{A_1}{\varphi}\frac{d^3f}{d\eta^3} + A_2\left(f\frac{d^2f}{d\eta^2} - \left(\frac{df}{d\eta}\right)^2\right) + \Lambda\beta\left(\frac{dF}{d\eta} - \frac{df}{d\eta}\right) + \frac{A_1}{\varphi}Da^{-1}\frac{df}{d\eta} = 0, \tag{20}$$

$$\left(\frac{dF}{d\eta}\right)^2 - f\frac{d^2f}{d\eta^2} + \beta\left(\frac{dF}{d\eta} - \frac{df}{d\eta}\right) = 0, \tag{21}$$

$$\left(\frac{A_3}{\varphi} + N_r\right)\frac{d^2\theta}{d\eta^2} + \Pr A_4\left(f\frac{d\theta}{d\eta} - 2\frac{df}{d\eta}\theta\right) + \Lambda\beta_T\gamma\Pr(\Phi - \theta) + \Lambda\beta_T\gamma\Pr E_c\left(\frac{dF}{d\eta} - \frac{df}{d\eta}\right)^2 = 0, \tag{22}$$

$$N_r\frac{d^2f}{d\eta^2} + \Pr\Lambda\gamma\left(F\frac{d\Phi}{d\eta} - 2\frac{dF}{d\eta}\Phi\right) - \beta_T\Pr\Lambda\gamma(\Phi - \theta) = 0, \tag{23}$$

with transformed boundary conditions are

$$\left.\begin{array}{l} f = V_c, \dfrac{\partial f}{\partial\eta} = d, \theta(\eta) = 1, \text{at} \quad \eta = 0, \\ \dfrac{df}{d\eta}\to 0, \dfrac{dF}{\partial\eta} \to 0, F = f, \theta\to 0, \Phi\to 0 \quad \text{as} \quad \eta\to\infty. \end{array}\right\}, \tag{24}$$

where

$$A_1 = \frac{\mu_{tnf}}{\mu_f}, A_2 = \frac{\rho_{tnf}}{\rho_f}, A_3 = \frac{\kappa_{tnf}}{\kappa_f}, A_4 = \frac{(\rho C_p)_{tnf}}{(\rho C_p)_f}.$$

in a mass number of dust particles are present is determined by $\Lambda = \frac{\rho_p}{\rho}$, with the particle phase density represented as $\rho_p = Nm, \beta = \frac{1}{|c|\tau_v}$ is the fluid-particle interaction variable with velocity dependence, parameter of the prandtl number is to be $\Pr = \frac{\nu\rho C_p}{k}$, suction/injection parameter is V_c, particular heat coefficient is $\gamma = \frac{c_m}{c_p}, \beta_T = \frac{1}{|c|\tau_T}$ is the temperature fluid-interaction component, in additionally the value of Eckert number is $Ec = \frac{c^2}{bc_p}, Da^{-1} = \frac{\nu_f}{K|c|}$ is the inverse Darcy number, $N_r = \frac{16\sigma^* T_\infty^3}{3\kappa\kappa_f}$ is the radiation parameter respectively. Moreover, d is set to such an extent that $d = 1$ represents the stretching sheet and $d = -1$ represents the shrinking sheet.

4. Solution of momentum equation for dusty and fluid flow phase

The exponential form solution provides the accurate analytical solution to eqns. (20) and (21) applied to the governing boundary conditions [20,39].

$$f(\eta) = V_c + d\left\{\frac{1 - exp(-\lambda\eta)}{\lambda}\right\}, F(\eta) = V_c + d\left\{\frac{1 - \alpha\, exp(-\lambda\eta)}{\lambda}\right\}, \tag{25}$$

It is necessary for it to correspond to the actual boundary limitations (24), in that λ should be strictly positive. whereas for, α denotes the stretching speed of the dust particles, no such limitation is required. It is currently unknown what the real values are for both λ and α. Consequently, the relationship is produced by the momentum equation for the fluid phase,

$$\frac{A_1}{\varphi}\lambda^2 - V_c\lambda A_2 - A_2 d + \Lambda\beta(\alpha - 1)\frac{A_1}{\varphi}Da^{-1} = 0, \tag{26}$$

momentum equation for the dust phase fluid as follows

$$\beta - V_c\lambda\alpha - d\alpha - \beta\alpha = 0, \tag{27}$$

by solving Eqn. (21) which gives as follows

$$\alpha = \frac{\beta}{\beta + V_c\lambda + d}, \tag{28}$$

substituting the value of Eqn. (28) in Eqn. (26) which gives the algebraic equation of degree three.

$$A\lambda^3 + B\lambda^2 - c\lambda - e = 0, \tag{29}$$

roots of the above algebraic equations are given below

$$\lambda_1 = -\frac{B}{3A} - \frac{2^{\frac{1}{3}}\left(-B^2 - 3Ac\right)}{3A\left(-2B^3 + 27A^2e + \sqrt{4\left(-B^2 - 3Ac\right)^3 + \left(\sqrt{-2B^2 - 9ABc + 27A^2e}\right)^2}\right)^{\frac{1}{3}}} + \left(\frac{-2B^3 - 9ABc + 27A^2e + \sqrt{4\left(-B^2 - 3Ac\right)^3 + \left(\sqrt{-2B^2 - 9ABc + 27A^2e}\right)^2}}{3 * 2^{\frac{1}{3}}A}\right), \tag{30}$$

$$\lambda_2 = -\frac{B}{3A} + \frac{(1+i)\left(-B^2 - 3Ac\right)}{3 * 2^{\frac{1}{3}}A\left(-2B^3 - 9ABc + 27A^2e + \sqrt{4\left(-B^2 - 3Ac\right)^3 + \left(\sqrt{-2B^2 - 9ABc + 27A^2e}\right)^2}\right)^{\frac{1}{3}}} - (1-i)\left(\frac{-2B^3 - 9ABc + 27A^2e + \sqrt{4\left(-B^2 - 3Ac\right)^3 + \left(\sqrt{-2B^2 - 9ABc + 27A^2e}\right)^2}}{3 * 2^{\frac{1}{3}}A}\right), \tag{31}$$

$$\lambda_3 = -\frac{B}{3A} + \frac{(1-i)\left(-B^2 - 3Ac\right)}{3 * 2^{\frac{1}{3}}A\left(-2B^3 - 9ABc + 27A^2e + \sqrt{4\left(-B^2 - 3Ac\right)^3 + \left(\sqrt{-2B^2 - 9ABc + 27A^2e}\right)^2}\right)^{\frac{1}{3}}} - (1+i)\left(\frac{-2B^3 - 9ABc + 27A^2e + \sqrt{4\left(-B^2 - 3Ac\right)^3 + \left(\sqrt{-2B^2 - 9ABc + 27A^2e}\right)^2}}{3 * 2^{\frac{1}{3}}A}\right), \tag{32}$$

where

$$\left.\begin{aligned} &A = \frac{A_1}{\varphi}, B = \frac{A_1}{\varphi}d + \frac{A_1}{\varphi}\beta - A_2{V_c}^2, \\ &c = 2A_2V_cd + A_2V_c\beta + \Lambda\beta V_c + \frac{A_1}{\varphi}V_cDa^{-1}, \\ &e = A_2d\beta + A_2d^2 + \Lambda\beta d + \frac{A_1}{\varphi}dDa^{-1} + \frac{A_1}{\varphi}\beta Da^{-1}, \end{aligned}\right\}, \tag{33}$$

moreover, using the formulae, the wall shears can be quickly estimated once the values of λ and α have been established,

$$\left.\begin{aligned} &\left(\frac{d^2f}{d\eta^2}\right)_{\eta=0} = -d\lambda, \\ &\left(\frac{d^2F}{d\eta^2}\right)_{\eta=0} = -d\alpha\lambda, \end{aligned}\right\}. \tag{34}$$

5. Thermal regions of fluid and dusty phases

The fluid phase temperature fields and the dusty fluids temperature fields are given a specific form [20,39].

$$\theta(\eta) = exp[-2\lambda\eta], \Phi(\eta) = \varphi\, exp[-2\lambda\eta], \tag{35}$$

where for the dusty fluid, the predicted wall temperature is Φ. These can be substituted into the energy equations in (22) and (23) to produce the polynomial equations

$$-2D\Pr A_4 - 2\left(\Pr V_cA_4 - 2\lambda\left(\frac{A_3}{\varphi} + N_r\right)\right)\lambda + d^2Ec\Lambda(-1+\alpha)^2 + \Lambda\beta\gamma\Pr(-1+\varphi) = 0, \tag{36}$$

$$Nr4\lambda^2 - 2\Pr\Lambda\gamma V_c\varphi\lambda - 2\Pr\Lambda\gamma\varphi d - \beta_T\Pr\Lambda\gamma\varphi + \beta_T\Pr\Lambda\gamma = 0, \tag{37}$$

After simplifying Eqn. (37) we have the following value of φ,

$$\text{that is } \varphi = \frac{N_r4\lambda^2 + \beta_T\Pr\Lambda\gamma}{\beta_T\Pr\Lambda\gamma + 2\Pr\Lambda\gamma V_c\lambda + 2\Pr\Lambda\gamma d\lambda}, \tag{38}$$

In order to compute the During the fluid as well as dust regimes, the efficiency of heat exchange, which is stated as

$$-\left(\frac{d\theta}{d\eta}\right)_{\eta} = 0 = 2\lambda, \tag{39}$$

$$-\left(\frac{d\Phi}{d\eta}\right)_{\eta=0} = 2\varphi\lambda,$$

6. Results and discussion

In the present work, it is studied how in the existence of porous stretching/shrinking surface has an effect on flow of unique/various two-phase dusty fluids and thermal situations. The governing equations are converted into ordinary differential equations using appropriate dimensionless variables, and the analytical solutions to these equations are then obtained. Additionally, look into the graphical influence of certain essential factors on the temperature distribution and velocity, few particular nanoparticles select to describe the present results (see Table 1).

Table 1
Properties of base fluid and nano particles numerical values [48–54,5354, 58–60].

Properties	H_2O	Silver (Ag)	SWCNTs	Graphene
$\rho(kgm^{-3})$	997.1	10500	2600	2200
$\kappa(wm^{-1}k^{-1})$	0.613	429	6000	5000
$C_p(JKg^{-1}K^{-1})$	4180	235	425	790

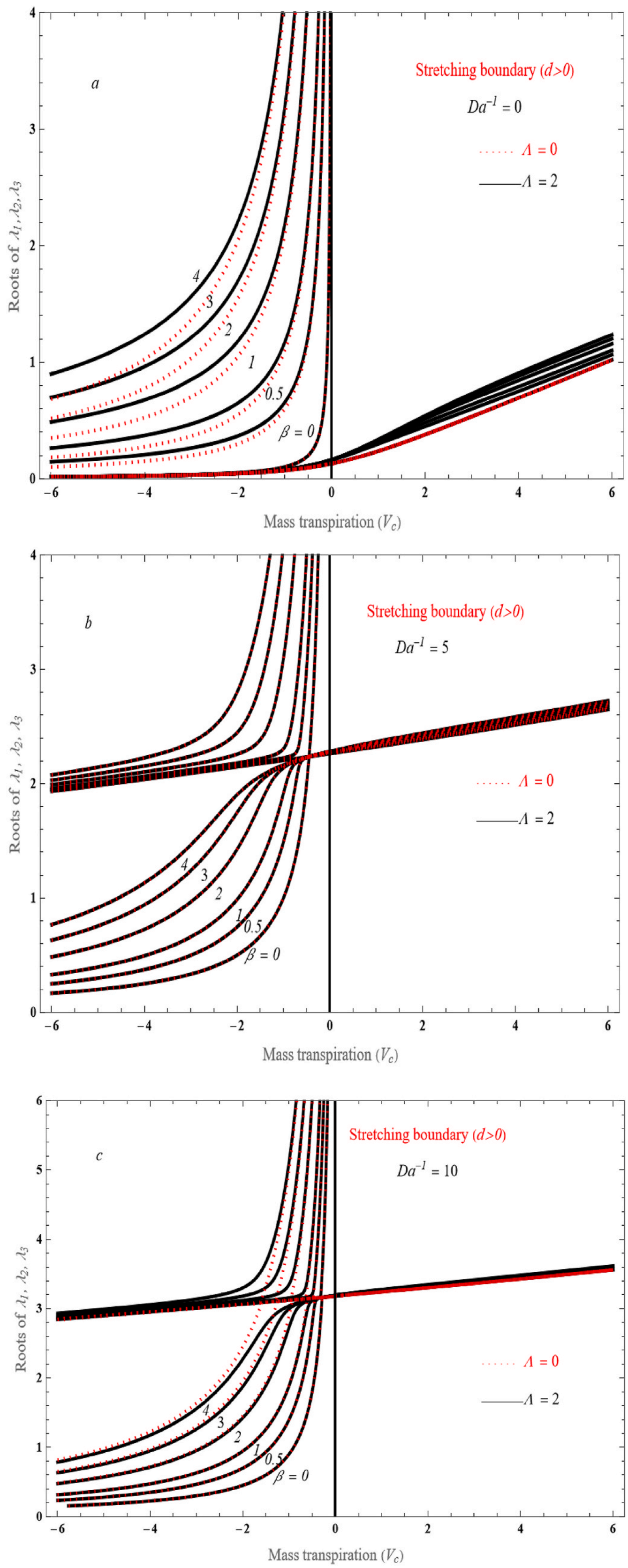

Fig. 2. Variations in the fluid particle interaction parameter $\beta = 0, 0.5, 1, 2, 3, 4$. are influenced by the range roots of the λ against mass transpiration along *(a)* $Da^{-1} = 0$ *(b)* $Da^{-1} = 5$ and *(c)* $Da^{-1} = 10$.

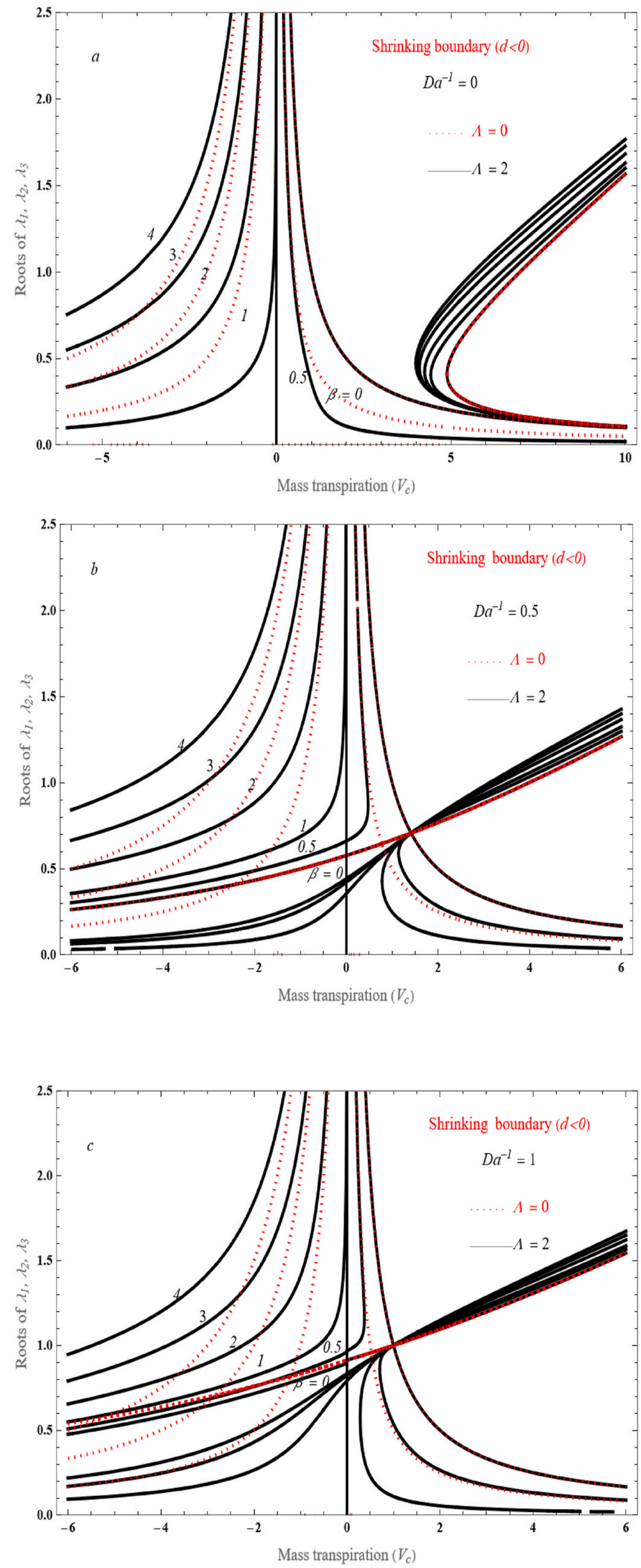

Fig. 3. Variations in the fluid particle interaction parameter $\beta = 0, 0.5, 1, 2, 3, 4$. are influenced by the range roots of the λ against mass transpiration with *(a)* $Da^{-1} = 0$ *(b)* $Da^{-1} = 0.5$ and *(c)* $Da^{-1} = 1$.

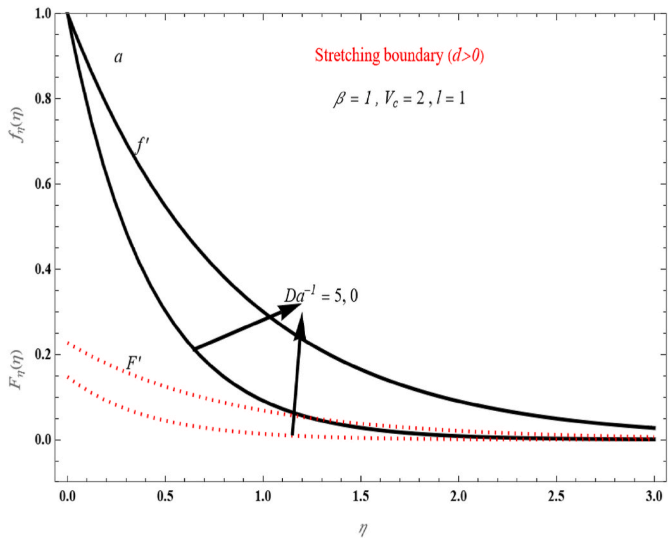

Fig. 4. Impact of velocity profile f_η of fluid and velocity profile F_η of particles for the stretching surface.

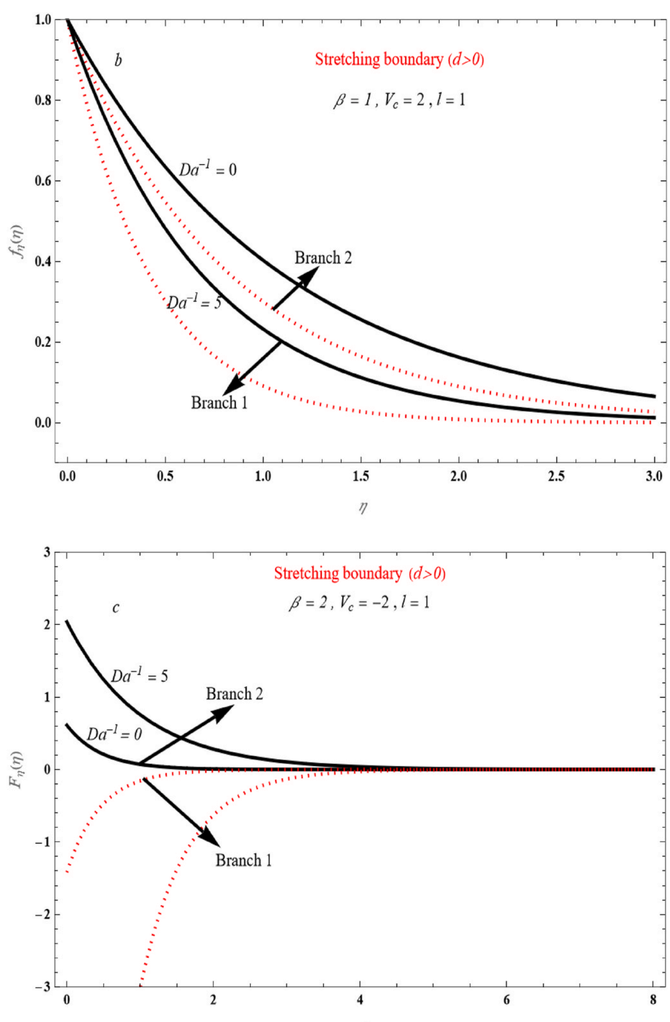

Fig. 5. Impact of velocity of fluid (a) f_η and (b) F_η velocities of the particles for the dual-solution stretching surface.

Fig. 2(a)-(c) illustrate the solution domains for the exponent λ against mass transpiration V_c values, when the stretching surface is taken into account with $\Lambda = 0$ and $\Lambda = 2$. at different values of Darcy number parameters $Da^{-1} = 0, 5, 10$. varying the values of fluid interaction parameter β. It appears that the exponent is a uniformly increasing function of V_c for all the given parameters, and also that the rising is further enhanced with Λ, and Da^{-1} increase.

When a surface is shrinking, Fig. 3(a)–(d) displays the solution domain λ as a function of mass transpiration V_c in case of a shrinking surface. For varying interaction parameter β with Darcy number at various values $Da^{-1} = 0, 0.5, 1$, with dust particle mass concentration $\Lambda = 0$ and $\Lambda = 2$. Despite the fact that both a rise and a decline can be seen in the wall suction velocities, the assessments of comparable velocities are uniformly improving.

The effect of the stretched surface regarding the phase velocity of both nanofluids and dust fluid as seen through Fig. 4. In the mass flow suction case, thickness of the momentum boundary layer is simultaneously diminished, resulting via decreased velocity of the ternary nanofluid as well as dust phase; hence there is only one solution is obtained.

According to Fig. 5(b)-(c), the fluid phase's velocity in Branch 1 is higher than the dusty fluids velocity, although in Branch 2, the ternary nanofluid phase velocity is less than dusty phase. The Darcy number value is enhanced as the velocity profile becomes linear.

Fig. 6(a)–(c) Illustrates How the stretching surface unique/distinctive two-phase temperature fields derived from Eqn. (13) will be have.

Fig. 7(a-c) shows how the shrinking surface affected both the fluid and dusty fluid velocity distribution. In Fig. 7(a), the suction case is depicted. Fig. 7(a), It has been shown that as the suction improved, the fluid and the dusty velocity profiles rise. Unfortunately, since the Darcy number acts to diminish the increase of the boundary layer, the physical reality of this behavior is in discussion, as observed in Fig. 7(a) as observed Fig. 6(b) and (c), the second branches for fluid injection do not always respond to physical assumptions. Branch 2 solutions are sensitive to hydrodynamic disturbances due to their thicker boundary layers.

Fig. 8(a)–(d) shows the fluid and dust particle temperature fields in two phases as determined by Eqn. (13) which deals with a shrinking surface. It's also interesting to observe that all parameter values in the figures show points of coincidence; these points exist whenever $\alpha = 1$, when the velocities of the fluid as well as the dusty are equal.

This paper addresses the transfer of momentum and energy of a two-phase dusty ternary nanofluid flow over a porous stretching/shrinking sheet. For a viscous incompressible flow, the governing equations associated with the momentum and thermal fields are presented under the steady conditions as stated in the previous literature [20,39]. After applying the proper similarity transformations, a set of nonlinear ordinary differential equations is obtained representing the flow of fluid and dust phases as well as temperature field of fluid and dust phases. Assuming a solution of exponential type, the exact solution for the equations is devised, which manifests the main novelty of the paper as compared to the state of-art. Besides, we take into account the mass flow addition into the boundary layer together with the form of the shrinking surface. The graphs depict the velocity and the temperature. For the stretching sheet, the analysis is shown to lead to a unique solution if mass flow suction is considered. When the flow mass is added to the boundary layer, however, the mathematical analysis leads to multiple solutions has been observed. The study concludes with the following results:

- A dual solution is found to be a shrinking sheet.
- The strength of the particle interaction parameter increases with increasing the solution domain thickness.
- The velocity profile for two phases declines as Darcy number rises.
- The interaction of particle and fluid will increase as due to various values of Darcy number.

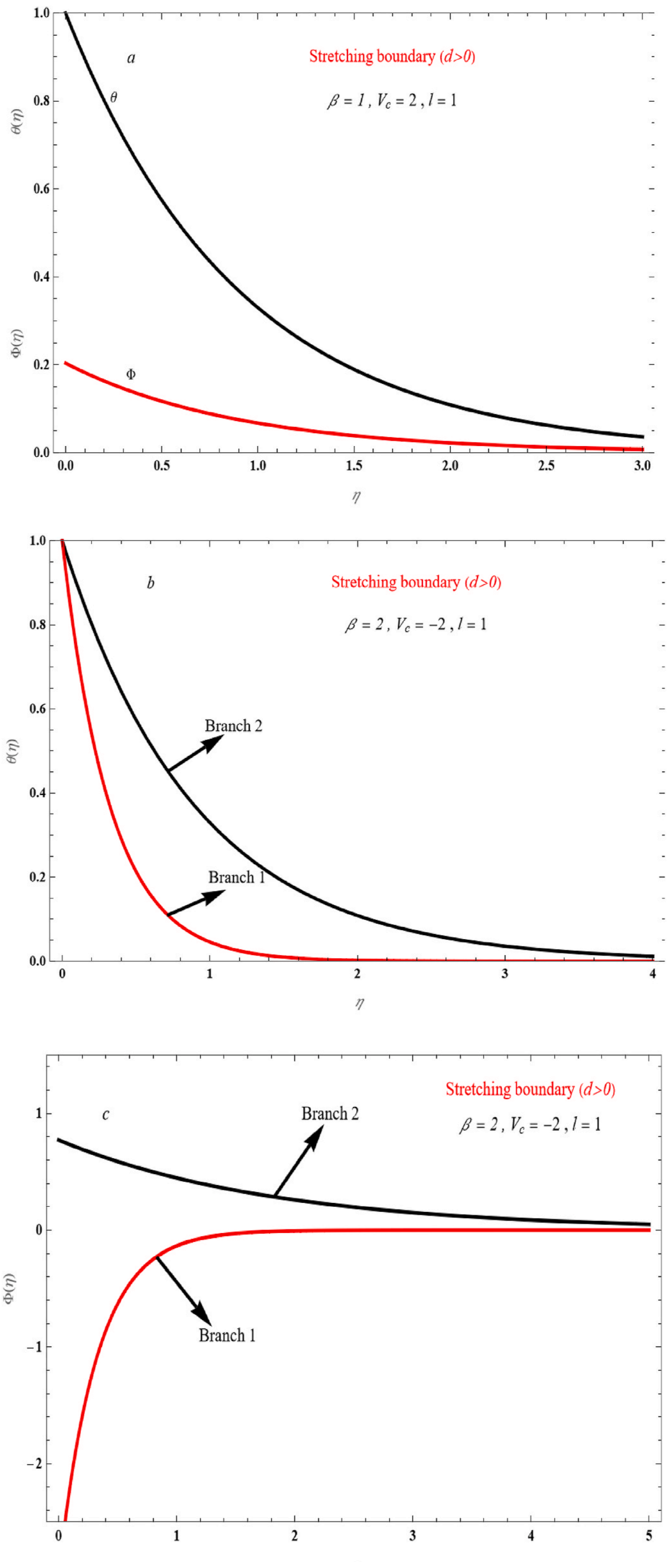

Fig. 6. Temperature profile for stretching surface. *(a)* unique solution of Φ and θ for $\Lambda = 1, \beta = 2, V_c = 2$, and $Da^{-1} = 0$. *(b)* two different solutions of θ when $\Lambda = 1, \beta = 2, V_c = -2$, and $Da^{-1} = 0$. *(c)* two different solutions of Φ for $\Lambda = 1, \beta = 2, V_c = -2$, and $Da^{-1} = 0$ with other variables are $\beta_T = 2$, $Nr = 0.1$, $Pr = 2$.

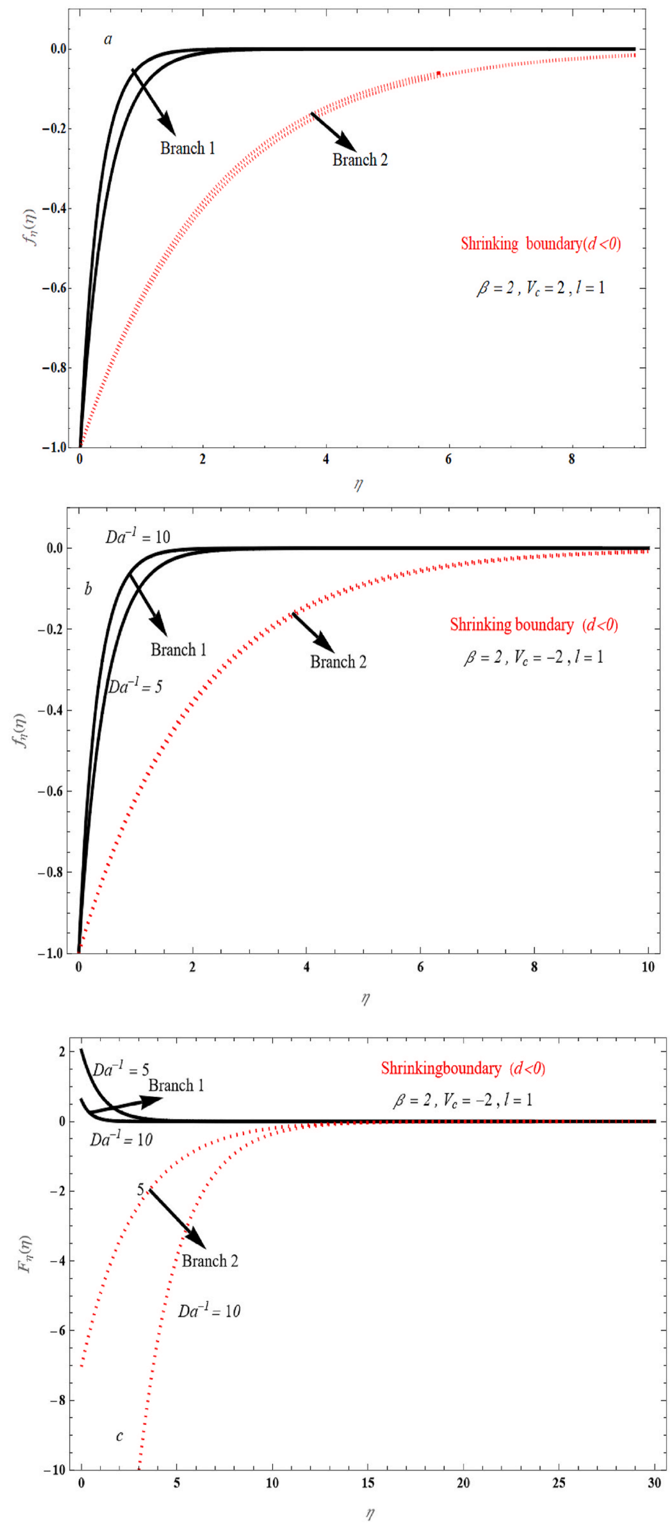

Fig. 7. Velocity profile f_η with velocity profile of the particles F_η for the shrinking sheet, (a) f_η to suction instance, *(b)–(c)* f_η and F_η forinjection instance.

- It depends mostly on the set of physical characteristics being taken into account as to whether branch 1 or branch 2 solutions are more cooled during a cooling procedure.
- If mass flow suction is taken into account, it is shown that the analysis produces a unique solution.

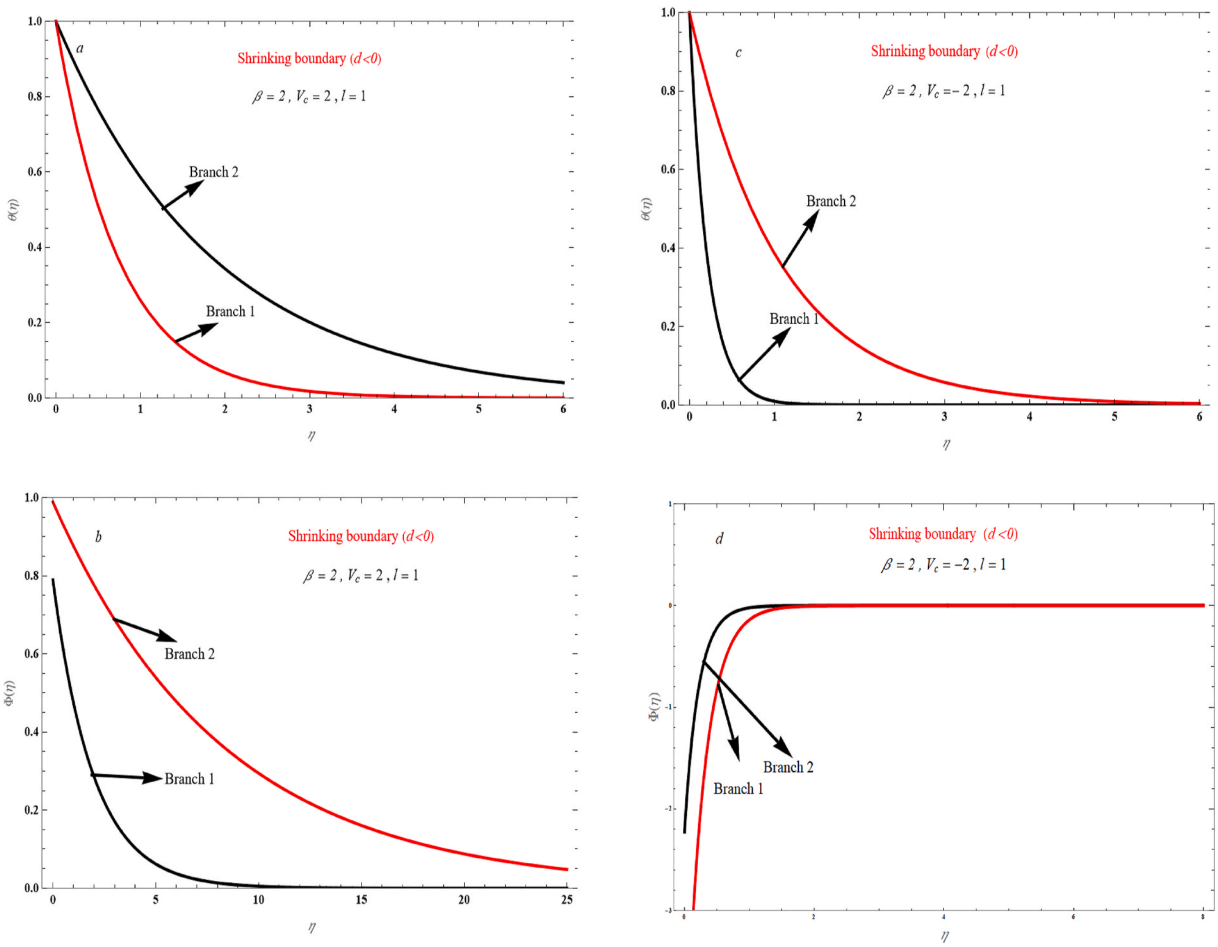

Fig. 8. Shrinking surface's response to temperature distributions the dual solutions of (a) and (b) for $\Lambda = 1, \beta = 1, V_c = 2$ and $Da^{-1} = 0$. *(c)* and *(d)* Two different solution of θ and Φ for $\Lambda = 1, \beta = 1, V_c = -2$ and $Da^{-1} = 0$. With $\beta_T = 2, \gamma = 1$, and $Da^{-1} = 2$.. 7. Concluding remarks.

Table 2
Comparision of the current research and relevant studies by other authors.

Related Works by Other Authors	Fluids	Value of λ
Turkyilmazoglu [20]	Non-Newtonian	$f(\eta) = s + D\frac{1-e^{-\lambda\eta}}{\lambda}, F(\eta) = s + D\frac{1-\Lambda e^{-\lambda\eta}}{\lambda}$ Where $\Lambda = \frac{\beta}{D+\beta+s\lambda}$.
Sneha [39]	Non-Newtonian	$f(\eta) = V_c + D\frac{1-e^{-\lambda\eta}}{\lambda}, F(\eta) = V_c + D\frac{1-\alpha e^{-\lambda\eta}}{\lambda}$ Where $\alpha = \frac{\beta_v}{D+\beta_v+V_c\lambda}$. Pr Present Present work Non-NewtonianPp Prese
Present work	Non-Newtonian	$f(\eta) = V_c + d\left\{\frac{1-exp(-\lambda\eta)}{\lambda}\right\}, F(\eta) = V_c + d\left\{\frac{1-\alpha\, exp(-\lambda\eta)}{\lambda}\right\}$ Where $\alpha = \frac{\beta}{\beta+V_c\lambda+d}$.

A number of preceding studies served as the limiting case for the current investigation:

i. $\lim\limits_{\substack{q_r \to 0, \\ \varphi \to 0.}}$ {Our results}→ {Results of Turkyilmazoglu et al. [20]}.

ii. In the presence of inclined MHD, and solid volume fraction $\varphi_3 = 0$, {Our results} → {Results of Sneha et al. [39]}.

Additionally, in a prospective future work, the particle phase slip velocity mechanism could be extended from the current analytical solutions to more particular cases like non-Newtonian fluid.

7. Validation

The research reveals the effect of radiation on dusty ternary nanofluid flow over a porous stretching/shrinking sheet with mass transpiration. In the absences of magnetic field $M = 0$, and solid volume fraction $\varphi_3 = 0$ leads to the results of Sneha et al. [39]. In the presence of magnetic field $M = 0$ and absences of $Da^{-1} = 0$, and $\varphi = 0$ the results leads to Turkyilmazoglu et al. [20]. The Comparision of the results are given in Table 2.

Author statement

T. Maranna – Calculation, equations, writing. U.S. Mahabaleshwar – comments, plotting, analysis. L.M. Perez – writing, corrections, plotting, comments. Hakan F. Öztop – Checking, literature, writing. G. Bognar – Literature, comments, checking.

Declaration of competing interest

The authors declare that they have no known competing financial interests or personal relationships that could have appeared to influence the work reported in this paper.

Data availability

No data was used for the research described in the article.

Acknowledgement

L.M.P. acknowledges partial financial support from ANID through Convocatoria Nacional Subvención a Instalación en la Academia Convocatoria Año 2021, Grant SA77210040.

References

[1] P.G. Saffaman, On the stability of flow of a dusty gas, J. Mech. 13 (1962) 120–129, https://doi.org/10.1017/S0022112062000555.
[2] B.C. Sakiadis, Boundary-layer behavior on continuous solid surface, Boundary layer equation for two-dimensional and axisymmetric flow, AIChE J. 7 (1961) 26–28, https://doi.org/10.1002/aic.690070108.
[3] D.H. Michael, D.A. Miller, Plane parallel flow of a dusty gas, Mathematika 13 (1966) 97–109, https://doi.org/10.1112/S0025579300004289.
[4] L.J. Crane, Flow past a stretching plate, Z. Angew. Math. Mech. 21 (1970) 645–647, https://doi.org/10.1007/BF01587695.
[5] S.U.S. Choi, J.A. Eastman, Enhancing thermal conductivity of fluids with nano-particles, Am. Soc. Mech. Eng. Fluids Eng. Div. FED. 231 (1995) 99–105. ANL/MSD/CP-84938.
[6] U.S. Mahabaleshwar, I.E. Sarris, A.A. Hill, G. Lorenzini, An MHD couple stress fluid due to perforated sheet undergoing linear stretching with heat transfer, Int. J. Heat Mass Tran. 105 (2017) 157–167, https://doi.org/10.1016/j.ijheatmasstransfer.2016.09.040.
[7] U.S. Mahabaleshwar, P.N.V. Kumar, M. Shermet, Magnetohydrodynamic flow of a nanofluid driven by a stretching/shrinking sheet with suction, Springer plus 5 (2016) 1–9, https://doi.org/10.1186/s40064-016-3588-0.
[8] U.S. Mahabaleshwar, K.N. Sneha, H.N. Haung, An effect of MHD and radiation on CNTs-water based nanofluid due to stretching sheet in a Newtonian fluid, Case Stud. Therm. Eng. 28 (2021), 101462, https://doi.org/10.1016/j.csite.2021.101462.
[9] T. Anusha, H.N. Haung, U.S. Mahabaleshwar, Two dimensional unsteady stagnation point flow of Casson hybrid nanofluid over a permeable flat surface and heat transfer analysis with radiation, J. Taiwan Inst. Chem. Eng. 127 (2021) 79–91, https://doi.org/10.1016/j.jtice.2021.08.014.
[10] J. Buongiorno, Convective transport in nanofluid, J. Heat Tran. 128 (2006) 240–250, https://doi.org/10.1115/1.2150834.
[11] R.K. Tiwari, M.K. Das, Heat transfer argumentation in a two sided lid driven differentially heated square cavity utilizing nanofluids, Int. J. Heat Mass Tran. 50 (2007) 2002–2018, https://doi.org/10.1016/j.ijheatmasstransfer.2006.09.034.
[12] I.L. Animasaun, S.J. Yook, T. Muhammed, A. Mathew, Dynamics of ternary hybrid nanofluid subjected to magnetic flux density and heat source/sink on a convectively heated surface, J. surf and Interf. 28 (2022), 101654, https://doi.org/10.1016/j.surfin.2021.101654.
[13] S. Manjunatha, V. Puneeth, B.J. Gireesha, A. J, Chamka, Theoretical study of convective heat transfers in ternary nanofluid flowing past a stretching sheet, J. Appl. Comput. Mech. 8 (2022) 1279–1286, https://doi.org/10.22055/JACM.2021.37698.3067.
[14] S. Saleem, I.L. Animasaun, S.J. Yook, Q.M.A. Mdallal, N.A. Shah, M. Faisal, Insight into the motion of water converging three kinds of nanoparticles on a horizontal surface; significance of thermos-migration and Brownian motion of different nano particle, Surface. Interfac. 30 (2022), 101854, https://doi.org/10.1016/j.surfin.2022.101854.
[15] U.S. Mahabaleshwar, T. Anusha, M. Hatami, The MHD Newtonian hybrid nanofluid flow and mass transfer analysis due to super-linear stretching sheet embedded in porous medium, Sci. Rep. 11 (1) (2021) 1–17, https://doi.org/10.1038/s41598-021-01902-2.
[16] M. Sheikholeslami, M. Hatami, D.D. Ganji, Micropolar fluid flow and heat transfer in a permeable channel using analytical method, J. Molecular liquids. 194 (2014) 30–36, https://doi.org/10.1016/j.molliq.2014.01.005.
[17] M. Hatami, D.D. Ganji, Natural convection of sodium alginate(SA) non-Newtonian nanofluid between two verticle flat plates by analytical and numerical methods, Case Stud. Therm. Eng. 2 (2014) 14–22, https://doi.org/10.1016/j.csite.2013.11.001.
[18] P.G. Siddheshwar, U.S. Mahabaleshwar, Effect of radiation and heat source on MHD flow of a viscoelastic liquid and heat transfer over a stretching sheet, Int. J. Nonlinear Mech. 40 (2005) 807–820, https://doi.org/10.1016/j.ijnonlinmec.2004.04.006.
[19] P.G. Siddheshwar, A. Chan, U.S. Mahabaleshwar, Suction-induced magnetohydrodynamics of a viscoelastic fluid over a stretching surface within a porous media, IMA J. Appl. Math. 79 (2014) 445–458, https://doi.org/10.1093/imamat/hxs074.
[20] M. Turkyilmazoglu, Magnetohydrodynamic two-phase dusty fluid flow and heat model over deforming isothermal surfaces, Phys. Fluids 29 (2017), 013302, https://doi.org/10.1063/1.4965926.
[21] S. Naramgari, C. Sulochana, MHD flow of dusty nanofluid flow over a stretching surface with volume fraction of dust particles, Ain Shams Eng. J. 7 (2016) 709–716, https://doi.org/10.1016/j.asej.2015.05.015.
[22] P.N.V. Kumar, U.S. Mahabaleshwar, N. Swaminathan, G. Lorenzini, Effect of MHD and mass transpiration on a viscous liquid flow past porous stretching sheet with heat transfer, J. Eng. Thermophys. 30 (2021) 404–419, https://doi.org/10.1134/S1810232821030061.
[23] Y. Gao, N. Chakraborty, T.D. Dunstan, N. Swaminathan, Assessment of Reynolds averaged Navier-Stokes modeling of scalar dissipation rate transport in turbulent oblique premixed flames, Combust. Sci. Technol. 187 (2015), https://doi.org/10.1080/00102202.2015.1035372.
[24] A.R. Al-Obaidi, J. Alhamid, The effect of different twisted tape inserts configurations on fluid flow characteristics, pressure drop, thermo-hydraulic performance and heat transfer enhancement in the 3D circular tube, Int. J. Ambient Energy 44 (2023) 57–72, https://doi.org/10.1080/01430750.2022.2091023.
[25] A.R. Al-Obaidi, Thermal flow and heat performance analyses in circular pipe using different twisted tape parameters based on design of experiments, Heat Transf 51 (2022) 7202–7232, https://doi.org/10.1002/htj.22641.
[26] A.R. Al-Obaidi, Characterization of internal thermohydraulic flow and heat transfer improvements in a three-dimensional circular corrugated tube surfaces based on numerical simulation and design of experiment, Heat Transf 51 (2022) 4688–4713, https://doi.org/10.1002/htj.22519.
[27] A.R. Al-Obaidi, J. Alhamid, H.A. Khalaf, Effect of different corrugation interruption parameters on thermohydrodynamic characteristics and heat transfer performance of 3D three-dimensional corrugated tube, Case Stud. Therm. Eng. 32 (2022), 101879, https://doi.org/10.1016/j.csite.2022.101879.
[28] A.R. Al-Obaidi, Investigation of thermal flow structure and performance heat transfer in three dimensional circular pipe using twisted tape based on Taguchi method analysis, Heat Transf 51 (2022) 1649–1667, https://doi.org/10.1002/htj.22368.
[29] A.R. Al-Obaidi, J. Alhamid, Investigation of the effect of various corrugated pipe configurations on thermo-hydraulic flow and enhancement of heat transfer performance with the development of different correlations, Int. J. Therm. Sci. 176 (2022), 107528, https://doi.org/10.1016/j.ijthermalsci.2022.107528.
[30] A.R. Al-Obaidi, I. Chaer, Flow field structure, characteristics of thermo-hydraulic and heat transfer performance analysis in a three dimensions' circular tube with different ball turbulators configurations, Arabian J. Sci. Eng. (2021), https://doi.org/10.1007/s13369-021-05943-7.
[31] A.R. Al-Obaidi, J. Alhamid, Q. Saleh, Analysis on flow structure and improvements of heat transfer in 3D circular tube with varying axial groove turbulators configurations, Heat Transf 50 (2021) 7333–7348, https://doi.org/10.1002/htj.22231.
[32] A. Shafiq, A.B. Colak, T.N. Sindhu, Q.M. Al-Mdallal, T. Abdelijawad, Estimation of unsteady hydromagnetic williamson fluid flow in a radiative surface through numerical and artificial neural network modelling, Sci. Rep. 11 (2021), 14509, https://doi.org/10.1038/s41598-021-93790-9.
[33] A. Shafiq, A.B. Colak, T.N. Sindhu, Construction of neural network based intelligent computing for treatment of Darcy Forchheimer sisko nanofluid flow with Rosseland's radiative process, Heat Tran. Res. 54 (2023) 77–98, https://doi.org/10.1615/Heat TransRes.2023046617.
[34] B. Souayeh, Simultaneous features of CC heat flux on dusty ternary nanofluid (Graphene+Tungsten+Zirconium oxide) through a magnetic field with slippery conditions, Mathematics 11 (2023) 554, https://doi.org/10.3390/math11030554.
[35] N.C. Roy, A.H. Hossain, I. Pop, Flow and heat transfer of MHD dusty hybrid nanofluids over a shrinking sheet, Chin. J. Phys. 77 (2022) 1342–1356, https://doi.org/10.1016/j.cjph.2021.12.012.
[36] F.M.S. Noorzehan, A. Anati, M. Syahira, M. Radiah, A.J. Nurul, Boundary layer of a dusty fluid flow over a stretching sheet, Int. J. Eng. Technol. 7 (2018) 462–464, https://doi.org/10.14419/ijet.v714.30.22368.
[37] A.B. Vishalakshi, T. Maranna, U.S. Mahabaleshwar, D. Laroze, An effect of MHD on Non-Newtonian fluid flow over a porous stretching/shrinking sheet with heat transfer, Appl. Sci. 12 (2022) 4937, https://doi.org/10.3390/app12104937.

[38] T. Maranna, K.N. Sneha, U.S. Mahabaleshwar, I.E. Sarris, T.E. Karakasidis, An effect of radiation and MHD Newtonian fluid over a stretching/shrinking sheet with CNTs and mass transpiration, Appl. Sci. 12 (2022) 5466, https://doi.org/10.3390/app12115466.

[39] K.N. Sneha, U.S. Mahabaleshwar, R. Bennacer, M.E.L. Ganaoui, Darcy Brinkmann equations for hybrid dusty Nanofluid flow with heat transfer and Mass Transpiration, Comput. Times 9 (2021) 118, https://doi.org/10.3390/computation9110118.

[40] T. Anusha, U.S. Mahabaleshwar, Y. Sheikhnejad, An MHD of nanofluid flow over a porous stretching/shrinking plate with mass transpiration and Brinkmann ratio, Transport Porous Media 142 (2021) 333–352, https://doi.org/10.1007/s11242-021-01695-y.

[41] J. Singh, U.S. Mahabaleshwar, G. Bognár, Mass transpiration in nonlinear MHD flow due to porous stretching sheet, Sci. Rep. 9 (2019), 18484, https://doi.org/10.1038/s41598-019-52597-5.

[42] T. Maranna, K.N. Sneha, U.S. Mahabaleshwar, B. Souayeh, An impact of heat and mass transpiration on magnetohydrodynamic viscoelastic fluid past a permeable stretching/shrinking sheet, Heat Transf (2022) 1–18, https://doi.org/10.1002/htj.22782.

[43] U.S. Mahabaleshwar, T. Maranna, F. Sofos, Analytical investigation of an incompressible viscous laminar Casson fluid flow past a stretching/shrinking sheet, Sci. Rep. 12 (2022), 18404, https://doi.org/10.1038/s41598-022-23295-6.

[44] M. Sahu, J. Sarkar, Steady-state energentic and exergetic performance of single phase natural circulation loop with hybrid nanofluids, J. Heat Tran. 141 (8) (2019), 082401, https://doi.org/10.1115/1.4043819.

[45] A.S. Nehad, I.L. Animasaun, A. Wakif, O.K. Koriko, R. Sivaraj, K.S. Adegbie, Z. Abdelmalek, H. Vaidya, A.F. Ijirimoye, K.V. Prasad, Significance of suction and dual stretching on the dynamics of various hybrid nanofluid: comparative analysis between type I and type II models, Phys. Scripta 95 (9) (2020), 095205, https://doi.org/10.1088/1402-4896/aba8c6.

[46] B. Takabi, S. Saleh, Augmentation of the heat transfer performance of a sinusoidal corrugated enclosure by employing hybrid nanofluid, Advanced, Mech. Eng. 16 (2014), 147059, https://doi.org/10.1155/2014/147059.

[47] K. Kalidasan, L.R. Velkennedy, P.R. Kanna, Laminar natural convection of copper-titania/water hybrid nanofluid in an open ended – C- shaped enclosure with an Isothermal block, J. Mol. Liq. 246 (2017) 251–258, https://doi.org/10.1016/j.molliq.2017.09.071.

[48] L.T. Benos, N.D. Polychronopoulos, U.S. Mahabaleshwar, G. Lorenzini, I.E. Sarris, Thermal and flow investigation of MHD natural convection in a nanofluid saturated porous enclosures: an asymptotic analysis, J. Ther Anal calorim. 143 (2021) 751–765, https://doi.org/10.1007/s10973-019-09165-w.

[49] C. Kleinstreuer, Y. Feng, Experimental and theoretical studies of nanofluid thermal conductivity enhancement: a review, Nanoscale Res. Lett. 6 (2011) 229, https://doi.org/10.1186/1556-276X-6-229.

[50] H. Liu, I.L. Animasaun, N.A. Shah, O.K. Koriko, B. Mahanthesha, Further discussion on the significance of quartic auto catalysis on the dynamics of water conveying 47nm alumina and 29 nm cupric particles, Arab. J. sci. Eng. 45 (7) (2016) 5977–6004, https://doi.org/10.1007/s13369-020-04610-7.

[51] T. Hayat, S. Qayyum, M. Imtiaz, A. Slaedi, Comparative study of silver and copper water nanofluids with mixed convection and non-linear thermal radiation, Int. J. Heat Mass Tran. 102 (2016) 723–732, https://doi.org/10.1016/j.ijheatmasstransfer.2016.06.059.

[52] T. Maranna, U.S. Mahabaleshwar, M.I. Kopp, An impact of Marangoni convection and radiation on flow of ternary nanofluid in a porous medium with mass transpiration, J. Appl. Comput. Mech. 9 (2023) 487–497, https://doi.org/10.22055/JACM.2022.41405.3748.

[53] F. Selimefendigil, H.F. Oztop, Thermal management for conjugate heat transfer of curved solid conductive panel coupled with different cooling systems using non-Newtonian power law nanofluid applicable to photovoltaic panel systems, Int. J. Therm. Sci. 173 (2022), 107390, https://doi.org/10.1016/j.ijthermalsci.2021.107390.

[54] F. Selimefendigil, H.F. Oztop, Impacts of using an elastic fin on the phase change process under magnetic field during hybrid nanoliquid convection through a PCM-packed bed system, 106958, Int. J. Mech. Sci. 216 (2022) 15, https://doi.org/10.1016/j.ijmecsci.2021.106958.

[55] U.S. Mahabaleshwar, T. Maranna, L.M. Perez, S.N. Ravichandra Nayakar, An effect of magnetohydrodynamic and radiation on axisymmetric flow of non-Newtonian fluid past a porous shrinking/stretching surface, J. Magn. Magn Mater. 571 (2023), 170538, https://doi.org/10.1016/j.jmmm.2023.170538.

[56] T. Maranna, U.S. Mahabaleshwar, L.M. Perez, O. Manca, Flow of viscoelastic ternary nanofluid over a shrinking porous medium with heat source/sink and radiation, Therm. Sci. Eng. Prog. 40 (2023), 101791, https://doi.org/10.1016/j.tsep.2023.101791.

[57] B.J. Gireesha, G.S. Roopa, C.S. Bagewadi, Boundary layer flow of an unsteady dusty fluid and heat transfer over a stretching/shrinking sheet with Non-Newtonian heat source/sink, Eng. J. 3 (2011) 726–735, https://doi.org/10.4236/eng.2011.37087.

[58] A. Jaafar, A. Jamaludin, N.A.A.M. Nasir, R. Nazar, I. Pop, MHD opposing flow of Cu-TiO_2 hybrid nanofluid under an exponentially stretching/shrinking surface embedded in porous media with heat source and slip impacts, Results Eng 17 (2023), 101005.

[59] R. Akhter, M.M. Ali, MdM. Billah, MdN. Uddin, hybrid-nanofluid mixed convection in square cavity subjected to oriented magnetic field and multiple rotating rough cylinders, Results Eng 18 (2023), 101100.

[60] S. Dinarvand, H. Berrehal, H. Tamim, G. Sowmya, S. Noeiaghadam, M. Abdollahzadeh, Squeezing flow of aqueous CNTs-Fe_3O_4 hybrid nanofluid through mass-based approach: effect of heat source/sink, nanoparticle shape, and an oblique magnetic field, Results Eng 17 (2023), 100976.